



*Supplement of*

## **Towards an efficient storm surge and inundation forecasting system over the Bengal delta: chasing the Supercyclone Amphan**

**Md. Jamal Uddin Khan et al.**

*Correspondence to:* Md. Jamal Uddin Khan ([jamal.khan@legos.obs-mip.fr](mailto:jamal.khan@legos.obs-mip.fr))

The copyright of individual parts of the supplement might differ from the article licence.

## 1 Bathymetry

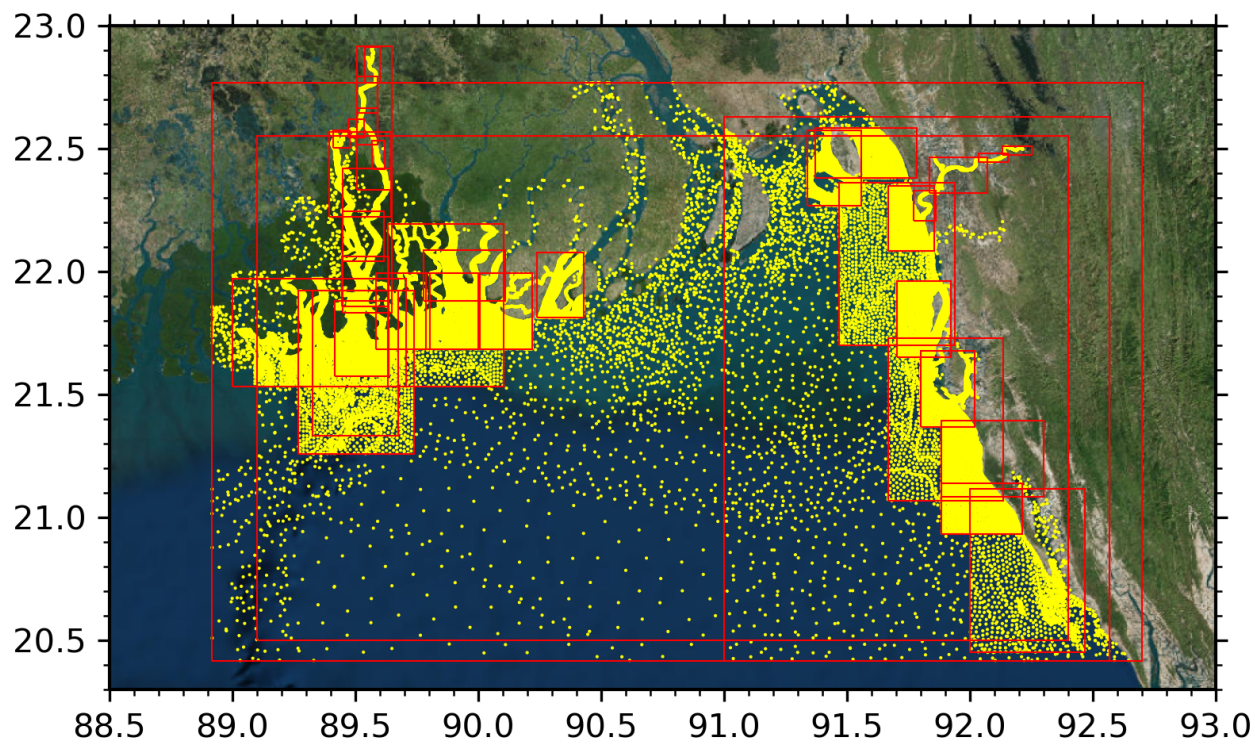


**Figure S1.** Newly digitized sounding points from Bangladesh Navy charts (in yellow) (Khan et al., 2019). The red boxes show the individual chart outlines. The background is a RGB image composite derived from B2, B3, and B4 channels of Sentinel-2.

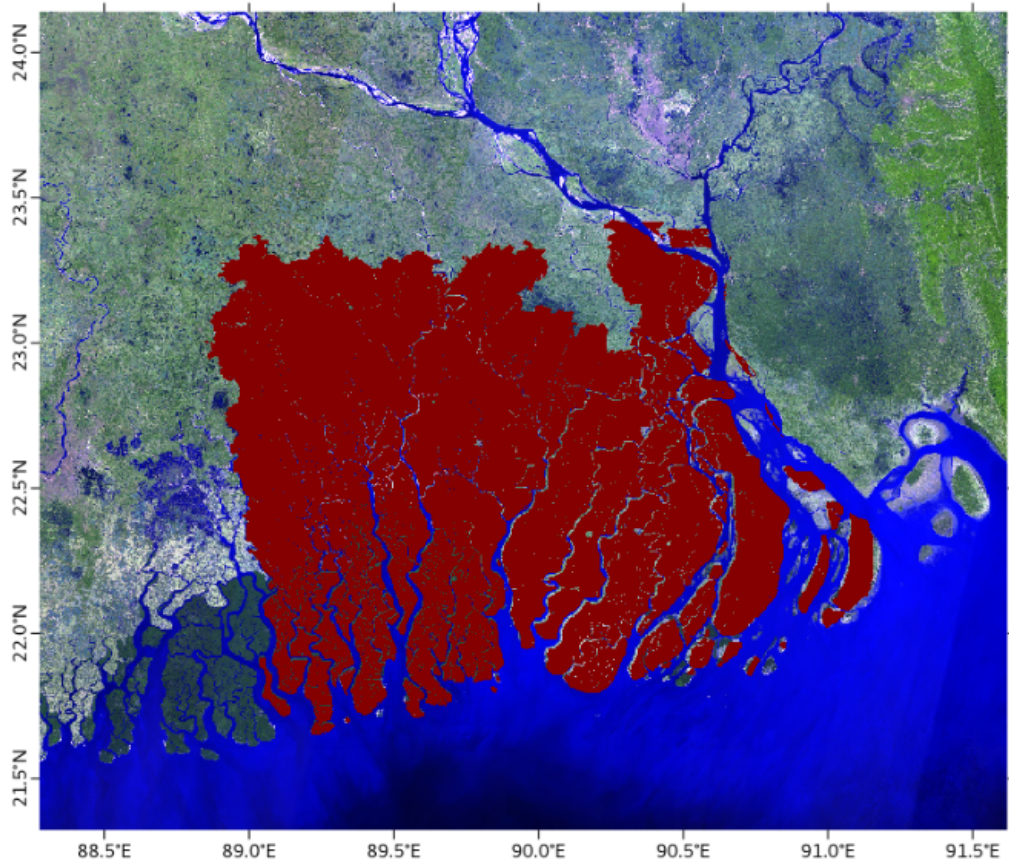


**Figure S2.** Extent of the 50 m resolution inland topography dataset (in red). The background is a false-colour image composite derived from B12, B11, and B4 channels of Sentinel-2.

## 2 Tide model validation

Our tidal model is validated at 7 tide gauge locations, around the Bengal delta (See Table S1). We have used complex error as the performance indicator (Mayet et al., 2013). The harmonic analysis is done using the Tidal toolbox developed at LEGOS (Allain, 2016). The modulus of the complex difference defines the complex error for a tidal constituent.

$$|\Delta z| = |A_m e^{i\phi_m} - A_o e^{i\phi_o}| \quad (S1)$$

Where  $A$  and  $\phi$  are the amplitude and phase (in radians) respectively, of the tidal harmonics. The subscript denotes the model ( $m$ ) and observation ( $o$ ). The total error of all the constituent at one location is calculated as the squared root of half of the squared sum.

$$\sigma_s = \sqrt{\frac{1}{2} \sum_N |\Delta z|^2} \quad (S2)$$

Along the coast of Bengal delta, only four of the constituents - M2, S2, K1, and O1 are found to contribute significantly to the tidal energy (Sindhu and Unnikrishnan, 2013). As in many cases, information for other tidal harmonics is not available, only these four constituents are considered for calculating the total complex error at a location.

A comparison of the complex error between the global models and the model presented here is shown in Table S1. Amplitudes ( $A$ ) and errors are in centimeter, phase ( $\phi$ ) is in degrees. Hooghly River, Diamond Harbour, Garden Reach and Chandpur are not represented in global tidal models (FES, GOT, and TPXO) due to their location in far upstream.

**Table S1.** Performance of tidal model at tide-gauge locations.

| Station   | Observation |          | FES2012-Hydro |          |       | FES2012   |          |       | GOT4.8    |          |       | TPXO7.2   |          |       | Krien et al. (2016) |          |           | This Model |          |       |             |
|---|-------------|----------|---------------|----------|-------|-----------|----------|-------|-----------|----------|-------|-----------|----------|-------|---------------------|----------|-----------|------------|----------|-------|-------------|
|   | $A_0$       | $\phi_0$ | $A_m$         | $\phi_m$ | Error | $A_m$     | $\phi_m$ | Error | $A_m$     | $\phi_m$ | Error | $A_m$     | $\phi_m$ | Error | $A_m$               | $\phi_m$ | Error     | $A_m$      | $\phi_m$ | Error |             |
| Sagar Roads<br>(88.0300°E,<br>21.6500°N)        | M2          | 140      | 116           | 142      | 99    | 42        | 137      | 104   | 29        | 113      | 113   | 27        | 132      | 104   | 28                  | 143      | 116       | 3          | 144.5    | 114.9 | 5.3         |
|   | S2          | 66       | 150           | 73       | 141   | 13        | 62       | 141   | 11        | 40       | 145   | 40        | 48       | 126   | 29                  | 62       | 155       | 7          | 62.4     | 153.3 | 5.2         |
|   | K1          | 15       | 262           | 17       | 256   | 2         | 16       | 253   | 3         | 14       | 277   | 14        | 14       | 258   | 1                   | 17       | 265       | 2          | 15.6     | 265.4 | 1.1         |
|   | O1          | 5        | 250           | 6        | 251   | 1         | 6        | 243   | 1         | 5        | 270   | 2         | 5        | 252   | 0.4                 | 6        | 248       | 1          | 5.7      | 251.6 | 0.8         |
|   | $\sigma_s$  |          |               |          |       | <b>31</b> |          |       | <b>22</b> |          |       | <b>27</b> |          |       | <b>29</b>           |          |           | <b>6</b>   |          |       |             |
| Diamond<br>Harbour<br>(88.1733°E,<br>22.1928°N) | M2          | 157      | 168           |          |       |           |          |       |           |          |       |           |          |       | 166                 | 161      | 21        | 142.3      | 165.6    | 15.9  |             |
|   | S2          | 68       | 210           |          |       |           |          |       |           |          |       |           |          |       | 68                  | 207      | 4         | 57.6       | 208.6    | 10.4  |             |
|   | K1          | 15       | 285           |          |       |           |          |       |           |          |       |           |          |       | 16                  | 284      | 1         | 13.2       | 286.3    | 1.8   |             |
|   | O1          | 7        | 258           |          |       |           |          |       |           |          |       |           |          |       | 5                   | 253      | 2         | 5.4        | 257.7    | 1.6   |             |
|   | $\sigma_s$  |          |               |          |       |           |          |       |           |          |       |           |          |       |                     |          | <b>15</b> |            |          |       | <b>13.6</b> |
| Hiron Point<br>(89.4780°E,<br>21.8169°N)        | M2          | 81       | 127           | 86       | 88    | 56        | 87       | 91    | 52        | 80       | 88    | 53        | 104      | 110   | 35                  | 81       | 115       | 17         | 99.9     | 115.0 | 26.7        |
|   | S2          | 34       | 159           | 45       | 121   | 28        | 40       | 122   | 24        | 37       | 118   | 25        | 37       | 136   | 14                  | 35       | 148       | 7          | 41.6     | 150.5 | 9.3         |
|   | K1          | 13       | 268           | 15       | 250   | 5         | 16       | 252   | 5         | 14       | 248   | 5         | 14       | 261   | 2                   | 15       | 265       | 2          | 15.0     | 265.7 | 1.7         |
|   | O1          | 5        | 258           | 6        | 244   | 2         | 6        | 238   | 2         | 5        | 244   | 1         | 5        | 256   | 0.3                 | 6        | 245       | 1          | 5.7      | 255.0 | 0.7         |
|   | $\sigma_s$  |          |               |          |       | <b>44</b> |          |       | <b>40</b> |          |       | <b>42</b> |          |       | <b>27</b>           |          |           | <b>13</b>  |          |       | <b>20.0</b> |
| Dhulasar<br>(90.2700°E,<br>21.8500°N)           | M2          | 73       | 158           | 58       | 114   | 52        | 80       | 117   | 53        | 79       | 117   | 54        | 86       | 121   | 51                  | 51       | 156       | 22         | 67.6     | 143.3 | 18.8        |
|   | S2          | 35       | 193           | 39       | 141   | 33        | 39       | 142   | 32        | 39       | 146   | 29        | 35       | 135   | 34                  | 20       | 194       | 15         | 28.5     | 179.6 | 9.8         |
|   | K1          | 13       | 286           | 15       | 262   | 6         | 16       | 256   | 8         | 15       | 260   | 6         | 15       | 255   | 8                   | 12       | 297       | 3          | 13.3     | 287.8 | 0.5         |
|   | O1          | 4        | 278           | 6        | 256   | 3         | 6        | 243   | 3         | 6        | 256   | 3         | 6        | 250   | 3                   | 5        | 280       | 1          | 5.6      | 273.8 | 1.6         |
|   | $\sigma_s$  |          |               |          |       | <b>44</b> |          |       | <b>44</b> |          |       | <b>44</b> |          |       | <b>44</b>           |          |           | <b>19</b>  |          |       | <b>15.0</b> |
| Charchanga<br>(91.0500°E,<br>22.2188°N)         | M2          | 96       | 234           | 110      | 202   | 57        | 115      | 208   | 50        | 97       | 204   | 49        | 84       | 154   | 103                 | 67       | 208       | 46         | 95.8     | 216.9 | 28.5        |
|   | S2          | 37.5     | 265           | 38       | 238   | 18        | 30       | 243   | 15        | 34       | 234   | 19        | 36       | 186   | 47                  | 27       | 241       | 17         | 36.6     | 250.3 | 9.5         |
|   | K1          | 13       | 304           | 17       | 298   | 4         | 16       | 300   | 4         | 7        | 314   | 6         | 16       | 272   | 8                   | 14       | 309       | 2          | 16.8     | 308.7 | 4.0         |
|   | O1          | 8        | 285           | 7        | 289   | 1         | 6        | 284   | 2         | 4        | 303   | 4         | 6        | 267   | 3                   | 8        | 289       | 0          | 8.1      | 293.1 | 1.1         |
|   | $\sigma_s$  |          |               |          |       | <b>43</b> |          |       | <b>37</b> |          |       | <b>37</b> |          |       | <b>80</b>           |          |           | <b>35</b>  |          |       | <b>21.5</b> |
| Chittagong<br>(91.8274 °E,<br>22.2434°N)        | M2          | 173      | 196           | 118      | 193   | 56        | 126      | 200   | 49        | 120      | 192   | 54        | 89       | 153   | 123                 | 156      | 198       | 18         | 149.2    | 194.8 | 24.1        |
|   | S2          | 64       | 229           | 41       | 230   | 23        | 33       | 236   | 31        | 43       | 227   | 21        | 40       | 160   | 62                  | 58       | 235       | 9          | 55.0     | 225.8 | 9.6         |
|   | K1          | 19       | 278           | 17       | 294   | 6         | 17       | 295   | 6         | 9        | 300   | 11        | 16       | 258   | 7                   | 20       | 289       | 4          | 19.1     | 284.9 | 2.3         |
|   | O1          | 8        | 263           | 7        | 285   | 3         | 6        | 280   | 3         | 4        | 289   | 5         | 6        | 252   | 2                   | 8        | 269       | 1          | 7.9      | 267.3 | 0.6         |
|   | $\sigma_s$  |          |               |          |       | <b>43</b> |          |       | <b>41</b> |          |       | <b>42</b> |          |       | <b>98</b>           |          |           | <b>14</b>  |          |       | <b>18.4</b> |
| Chandpur<br>(90.6385°E,<br>23.2344°N)           | M2          | 29.7     | 31.4          |          |       |           |          |       |           |          |       |           |          |       |                     |          |           |            | 33.6     | 333.7 | 30.7        |
|   | S2          | 10.5     | 62.3          |          |       |           |          |       |           |          |       |           |          |       |                     |          |           |            | 11.2     | 6.3   | 10.2        |
|   | K1          | 5.6      | 18.6          |          |       |           |          |       |           |          |       |           |          |       |                     |          |           |            | 5.4      | 21.9  | 0.7         |
|   | O1          | 3.4      | 12.9          |          |       |           |          |       |           |          |       |           |          |       |                     |          |           |            | 3.6      | 357.4 | 1           |
|   | $\sigma_s$  |          |               |          |       |           |          |       |           |          |       |           |          |       |                     |          |           |            |          |       |             |

### 3 Inundation

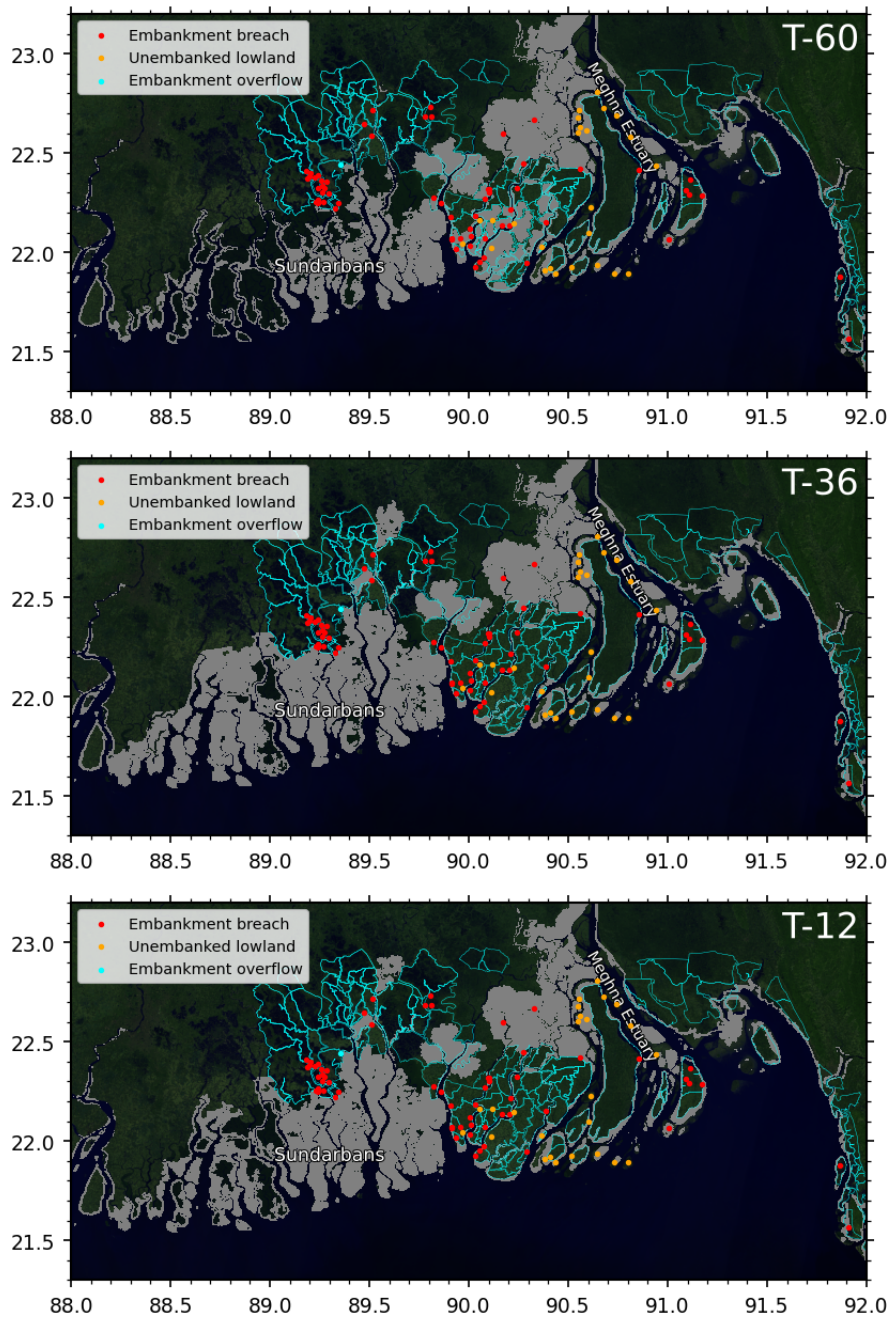


**Figure S3.** Same as Figure 9 for forecasts at T-60, T-36, and T-12 hours.

## References

- Allain, D. J.: TUGOm tidal toolbox, <ftp://ftp.legos.obs>, 2016.
- Khan, M. J. U., Ansary, M. N., Durand, F., Testut, L., Ishaque, M., Calmant, S., Krien, Y., Islam, A. K. M. S., and Papa, F.: High-Resolution Intertidal Topography from Sentinel-2 Multi-Spectral Imagery: Synergy between Remote Sensing and Numerical Modeling, *Remote Sensing*, 11, 2888, <https://doi.org/10.3390/rs11242888>, publisher: MDPI AG, 2019.
- Krien, Y., Mayet, C., Testut, L., Durand, F., Tazkia, A. R., Islam, A. K. M. S., Gopalakrishna, V. V., Becker, M., Calmant, S., Shum, C. K., Khan, Z. H., Papa, F., and Ballu, V.: Improved Bathymetric Dataset and Tidal Model for the Northern Bay of Bengal, *Marine Geodesy*, 39, 422–438, <https://doi.org/10.1080/01490419.2016.1227405>, publisher: Informa UK Limited, 2016.
- Mayet, C., Testut, L., Legresy, B., Lescarmonier, L., and Lyard, F.: High-resolution barotropic modeling and the calving of the Mertz Glacier, East Antarctica, *Journal of Geophysical Research: Oceans*, 118, 5267–5279, <https://doi.org/10.1002/jgrc.20339>, publisher: American Geophysical Union (AGU), 2013.
- Sindhu, B. and Unnikrishnan, A. S.: Characteristics of Tides in the Bay of Bengal, *Marine Geodesy*, 36, 377–407, <https://doi.org/10.1080/01490419.2013.781088>, publisher: Informa UK Limited, 2013.